

REC'D APR 3 1947

RM No. E7C26a

~~CLASSIFICATION CANCELLED~~

~~H. S. Dreyfus 6/5/53~~

~~NACA~~

~~OKL NACA change # 1425~~

Status: Restriction/Classification Cancelled

# RESEARCH MEMORANDUM

for the

Bureau of Aeronautics, Navy Department

ALTITUDE-WIND-TUNNEL INVESTIGATION OF R-4360-18

POWER-PLANT INSTALLATION FOR XR60 AIRPLANE

III - PERFORMANCE OF INDUCTION AND EXHAUST SYSTEMS

By David T. Dupree and W. Kent Hawkins

Aircraft Engine Research Laboratory  
Cleveland, Ohio

[Redacted]

[Redacted]

The information affecting the

Authority H. S. Dreyfus Date 12-6-50

Dir., Aeron. Research  
NACA

By OKL M. F. Schmidt see form # 493

**NATIONAL ADVISORY COMMITTEE  
FOR AERONAUTICS**

WASHINGTON

MARCH 28 1947

**FILE COPY**  
to be filed in the  
files of the  
Advisory Committee  
for Aeronautics  
Washington, D. C.

Restriction/  
Classification  
Cancelled

(11)

~~CLASSIFIED~~ ~~RESTRICTED~~ ~~CANCELLED~~

~~CLASSIFICATION CANCELLED~~

NATIONAL ADVISORY COMMITTEE FOR AERONAUTICS

RESEARCH MEMORANDUM

for the

Bureau of Aeronautics, Navy Department

ALTITUDE-WIND-TUNNEL INVESTIGATION OF R-4360-18

POWER-PLANT INSTALLATION FOR XR60 AIRPLANE

III - PERFORMANCE OF INDUCTION AND EXHAUST SYSTEMS

By David T. Dupree and W. Kent Hawkins

SUMMARY

A study has been made of the performance of the induction and the exhaust systems on the XR60 power-plant installation as part of an investigation conducted in the Cleveland altitude wind tunnel. Altitude flight conditions from 5000 to 30,000 feet were simulated for a range of engine powers from 750 to 3000 brake horsepower.

Slipstream rotation prevented normal pressure recoveries in the right side of the main duct in the region of the right inter-cooler cooling-air duct inlet. Total-pressure losses in the charge-air flow between the turbosupercharger and the intercoolers were as high as 2.1 inches of mercury. The total-pressure distribution of the charge air at the intercooler inlets was irregular and varied as much as 1.0 inch of mercury from the average value at extreme conditions. Total-pressure surveys at the carburetor top deck showed a variation from the average value of 0.3 inch of mercury at take-off power and 0.05 inch of mercury at maximum cruising power. The carburetor preheater system increased the temperature of the engine charge air a maximum of about 82° F at an average cowl-inlet air temperature of 9° F, a pressure altitude of 5000 feet, and a brake horsepower of 1240.

INTRODUCTION

An extensive investigation was conducted in the NACA Cleveland altitude wind tunnel at the request of the Bureau of Aeronautics,

~~CLASSIFICATION CANCELLED~~

Navy Department, to determine the performance characteristics of the R-4360-18 engine installation in the XR60 airplane. Altitude flight conditions from 5000 to 30,000 feet were simulated for a range of engine powers from 750 to 3000 brake horsepower and airspeeds from 100 to 175 miles per hour. The cooling characteristics and the performance of the engine are presented in references 1 and 2, respectively. The performance of the main duct, the charge-air system, the intercooler cooling-air system, and the exhaust system is discussed in this report.

Data for these duct systems were analyzed to determine the pressure and temperature gradients and to determine the pressure distribution at various cross sections of each duct. The performance of the intercooler cooling-air system was investigated to determine if a carburetor top-deck air temperature less than 100° F could be maintained with reasonable values of intercooler flap deflections and of cooling-air and charge-air pressure drops. The temperature-rise range of the preheater system for the charge air was also analyzed.

#### DESCRIPTION OF POWER-PLANT INSTALLATION

An XR60 nacelle mounted in a wing section was installed in the altitude wind tunnel, as shown in figure 1. The R-4360-18 engine was equipped with a General Electric Type BH-3 turbosupercharger and with a standard 19-foot four-blade Curtiss Electric propeller with 1 foot cut from the tip of each blade to give the necessary clearance in the tunnel. A more complete description of the engine and installation is given in references 1 and 2.

Engine charge air and intercooler cooling air entered a main duct at the lower front of the engine cowling, as shown in figures 1 and 2. Approximately 5 feet behind this entrance the main duct was divided into a group of smaller ducts.

Engine charge air flowed from a duct in the upper center of this group to the turbosupercharger inlet, from the turbosupercharger through two ducts to intercoolers on each side of the nacelle, then through two ducts leading to and joined at the carburetor top deck. Air was bled from the right duct at a location immediately after the turbosupercharger outlet for use in a cabin-air pressurization system. The flow from this cabin-air outlet was maintained at approximately 1800 pounds per hour in order to simulate the design flow. The ducts between the intercoolers and the

carburetor top deck were equipped with spring-loaded pressure-relief doors that were designed to open inward when the duct static pressure was lower than static pressure in the nacelle; this condition was anticipated at take-off power because the turbosupercharger is then windmilling.

Cooling air was supplied to the intercoolers by ducts located at opposite sides of the duct group and was discharged from the intercoolers to the free stream through outlets equipped with adjustable flaps.

Auxiliary ducts carried hot air from the exhaust collector-ring shrouds to the intercooler cooling-air ducts. Valves were provided to change from cooling air to hot air when heating of the charge air was desired. In figure 2 these valves are shown set for admission of hot air.

In the exhaust system (fig. 3), gas from the individual cylinders of each bank was collected by a manifold and taken to the collector ring. Two ducts connected the collector ring to the turbosupercharger inlets, where by-pass pipes branched off to the outlet of the turbosupercharger. Mechanically interconnected waste gates were installed in the by-pass pipes to control the flow through the turbosupercharger. Behind the turbosupercharger the exhaust gas was collected in a single duct and taken through the heat exchanger to the outlet. This heat exchanger was designed to provide heat for the wing de-icing and cabin-air systems. The exhaust outlet was a straight pipe directed to the rear of the nacelle and did not extend beyond the outer surface.

#### PROCEDURE

Pressure and temperature measurements were obtained at the various stations outlined in the following table:

Location	Total-pressure tubes	Static-pressure tubes	Thermo-couples
Main duct inlet	8		1
Charge-air system			
Inlet duct	5		1
Inlet of turbosupercharger	3		1
Outlet of turbosupercharger (L and R)	2		1
Inlet of intercooler (L and R)	5		2
Outlet of intercooler (L and R)	5		2
Carburetor top deck	10		4
Intercooler cooling-air system			
Inlet duct (L and R)	3		
Inlet of intercooler (L and R)	9		2
Outlet of intercooler (L and R)	9	4	2
Exhaust system			
Each cylinder port		1	
Collector ring		7	4
Gas inlet of turbosupercharger (L and R)		1	1
Gas inlet of heat exchanger		1	1
Gas outlet of heat exchanger		1	1

The power-plant installation was operated under simulated flight conditions of altitudes from 5000 to 30,000 feet and indicated airspeeds from 100 to 175 miles per hour. Most of the runs were made at an indicated airspeed of 150 miles per hour. Because the installation model was large relative to the 20-foot diameter of the tunnel test section, all runs were made at an inclination of the thrust axis of 0°.

The engine was operated over a range of brake horsepowers from 750 to 3000. Emphasis was placed on the following conditions: take-off power, 3000 brake horsepower at an engine speed of 2700 rpm; normal rated power, 2500 brake horsepower at 2550 rpm; and maximum cruising power, 1675 brake horsepower at 2230 rpm. Power-off tests were also made at an altitude of 10,000 feet for a range of indicated airspeeds from 100 to 175 miles per hour with the propeller removed to isolate the effects of the propeller slipstream.

The following coefficients are used in the investigation of the various duct systems:

$\frac{H-p_0}{q_c}$  pressure-recovery coefficient

$\frac{\Delta H}{q_c}$  pressure-drop coefficient

$\frac{\Delta D}{q_0}$  incremental-drag coefficient of the flaps

where

H local total pressure, pounds per square foot

$p_0$  free-stream static pressure, pounds per square foot

$q_c$  free-stream impact pressure as measured by pitot-static tube, pounds per square foot

$\Delta H$  total-pressure drop, pounds per square foot

$\Delta D$  increment of drag between minimum drag position of flaps and any other flap position, pounds

$q_0$  free-stream dynamic pressure,  $\frac{\rho V^2}{2}$ , pounds per square foot

$\rho$  air density, slugs per cubic foot

V true airspeed, feet per second

## RESULTS AND DISCUSSION

Main duct. - Patterns of pressure recovery at the main-duct inlet are shown in figure 4. A slight tendency toward a recovery higher than the average exists along the lower lip of the duct for both propeller-removed and propeller-operating conditions.

Variation of the total-pressure recovery at the main-duct inlet with brake horsepower, altitude, and indicated airspeed are shown in figure 5. An increase in the brake horsepower and a corresponding increase in propeller boost while the altitude and

the airspeed are held constant (fig. 5(a)) resulted in an increase in the pressure-recovery coefficients at the main-duct inlet. An increase in altitude at constant values of engine power and indicated airspeed (fig. 5(b)) increased the true airspeed and consequently reduced the effect of propeller boost on the total pressures at the main-duct inlet. The actual and relative values of the propeller boost decreased as the airspeed increased at constant altitude and power (fig. 5(c)).

The patterns of pressure recoveries at the entrance to the separate inlet ducts are shown in figure 6. The pressure recoveries obtained with the propeller removed were uniform across the duct entrances. When the propeller was operating, the pressure recovery on the right side of the ducts was relatively poor. This unbalance is attributed to the rotational component of the propeller slipstream.

The pressure recovery at the right intercooler-duct inlet was materially reduced by the unbalance in the main duct. The pressure-drop coefficients between the main-duct inlet and the intercooler-duct inlets are shown in figure 7. At high charge-air flows (high engine powers), the pressure-drop coefficient for the main duct in front of the right intercooler ranged between 0.2 and 0.3, whereas the loss encountered in the main duct in front of the left intercooler duct was negligible.

Charge-air system. - The distribution of pressure recovery at the charge-air duct inlet is shown in figure 8 to be quite uniform. This duct inlet is located in the upper center of the duct group and is unaffected by the inefficient pressure recovery on the right side.

Pressure and temperature gradients through the engine charge-air system are shown in figures 9 and 10, which give an over-all picture of the effect of engine power and altitude on pressures and temperatures in the various parts of the system. These data are useful only for their relative value because the magnitude of the pressure or temperature at any station downstream of the turbosupercharger is dependent on the adjustment of the waste-gate regulator, the operation of which was quite erratic throughout the investigation.

The performance of the intercooler system in maintaining the charge air at reasonable temperatures is best shown at more stable conditions than those of figures 9 and 10. Under more stable conditions, the intercooler system maintained the carburetor-deck temperature below 100° F with flaps faired at the following conditions: take-off power at a standard altitude of 5000 feet, and normal rated power at a standard altitude of 20,000 feet.

Losses of total pressure in various parts of the charge-air ducting are shown in figure 11. The greatest loss occurred in the ducts between the turbosupercharger and the intercoolers. This loss amounted to about 1.1 inches of mercury at a maximum cruising power and 2.1 inches of mercury at take-off power. Pressure distribution across the face of each intercooler entrance varied a maximum of about 1.0 inch of mercury from the average value. (See fig. 12.) The sharp bends in these ducts probably produced a stratification of the air flow, which caused this large pressure loss and poor pressure distribution. The possibility that the large pressure loss was caused by the bleeding of air from the right duct for the cabin-air system was not substantiated by the data. Average total pressures at the right and the left intercooler faces were usually almost equal, and the left turbosupercharger-outlet pressure was higher than the right by only 0.3 to 0.5 inch of mercury.

The distribution of total pressure at the carburetor top deck is shown in figure 13. At the high air flow encountered at take-off power, the total pressure varied as much as 0.3 inch of mercury from the average value (fig. 13(a)). At cruising powers, the total-pressure distribution was reasonably uniform, varying about 0.05 inch of mercury as seen in figure 13(b).

Intercooler system. - Pressure gradients through the intercooler cooling-air system are shown in figure 14. The pressure drop through the system was not materially affected by changes in altitude nor engine power but increased with intercooler flap deflection. The pressure recovery was lower at the right intercooler than at the left, caused by the unbalanced flow pattern in the main duct ahead of the cooling-air duct entrances.

Temperature gradients through the intercooler cooling-air system are shown in figure 15. Inasmuch as the difference in the temperatures of the air in the two branches of the system was negligible, the average values were plotted. An increase in altitude or brake horsepower caused an increase in temperature rise through the system.

The variation of intercooler-flap deflection from faired position to a deflection of  $34^\circ$  produced very little change in temperature rise of the cooling air as it passed through the intercoolers.

The pressure-recovery pattern of the cooling air at the intercooler-inlet face in figure 16 shows that the highest values



of the pressure-recovery coefficient occurred on the outer edge of each intercooler with the propeller either removed or operating. This effect was probably caused by the configuration of the ducts in front of the intercoolers. With the propeller removed, the left and the right intercoolers had approximately the same average pressure recovery; at rated power, the recovery at the left intercooler was higher than that at the right intercooler.

Cooling-air pressure drop through the intercooler is shown in figure 17. Little difference was indicated between propeller-removed and maximum-cruising conditions except at large flap openings where large air flows occurred. The decrease in the slope of the curves shows that the intercooler flaps became increasingly less effective at large deflections, a condition that was quite noticeable to the engine operator in the adjustment of carburetor-deck temperature.

The effect of intercooler-flap opening on the incremental-drag coefficient is also shown in figure 17. The intercooler flaps give the least amount of drag at the faired position. The effect of oil-cooler-flap and cowl-flap positions on the pressure drop through the intercoolers was found to be negligible, which showed that the intercooler flaps are located in a position where there is no interference from the other flap systems.

The characteristics of the intercoolers with the carburetor preheater system in operation are shown in figure 18. As shown by the low pressure recovery at the face of the intercoolers, most of the pressure drop across the intercoolers was induced by the action of the flaps. The average temperature rise of the engine charge air at a brake horsepower of 1240, an altitude of 5000 feet, and an average cowl-inlet air temperature of 9° F (a possible icing condition) was about 76° F at the initial flap deflection of 15° from faired position, and 82° F with wide open flaps.

Exhaust system. - Static pressures in the exhaust system were measured with tubes connected to static wall orifices. The values obtained were undoubtedly affected by pressure pulsations and occasionally by leaks in the tubing.

Variation of static pressure at individual cylinder exhaust ports is shown in figure 19, the greatest difference being about 5.5 inches of mercury at take-off power. Static-pressure gradients through the exhaust system are shown in figure 20 for a range of engine powers and altitudes. No noticeable static-pressure drop occurred in the duct from the outlet of the heat exchanger to free-stream conditions, as shown by the slightly negative static pressure at the heat-exchanger outlet.

## SUMMARY OF RESULTS

The following results were obtained from an investigation of the intake and the exhaust systems of the XR60 power-plant installation in the Cleveland altitude wind tunnel:

1. Slipstream rotation reduced pressure recoveries in the right side of the main duct in the region of the right intercooler cooling-air duct inlet.
2. Total-pressure losses in the charge-air flow were a maximum of 2.1 inches of mercury at take-off power in the ducting between the turbosupercharger and the intercoolers.
3. Total-pressure surveys of the charge air at the intercooler inlets showed a maximum variation from the average value of about 1.0 inch of mercury.
4. Total-pressure surveys at the carburetor top deck showed a variation from the average value of 0.3 inch of mercury at take-off power and 0.05 at maximum cruising power.
5. The carburetor preheater system increased the temperature of the charge air a maximum of 82° F at 1240 brake horsepower, a pressure altitude of 5000 feet, and an average cowl-inlet air temperature of 9° F.

Aircraft Engine Research Laboratory,  
National Advisory Committee for Aeronautics,  
Cleveland, Ohio.

*David T. Dupree*  
David T. Dupree,  
Mechanical Engineer.

*W. Kent Hawkins*  
W. Kent Hawkins,  
Aeronautical Engineer.

Approved:

Alfred W. Young,  
Mechanical Engineer.

Abe Silverstein,  
Aeronautical Engineer.

r1

## REFERENCES

1. Kuenzig, John K., and Moore, Stanley H.: Altitude-Wind-Tunnel Investigation of the R-4360-18 Power-Plant Installation for XR60 Airplane. I - Engine-Cooling Characteristics. NACA RM No. E7A15, Bur. Aero., 1947.
2. Meyer, Carl L., and Berdysz, Joseph J.: Altitude-Wind-Tunnel Investigation of the R-4360-18 Power-Plant Installation for XR60 Airplane. II - Power-Plant Performance. NACA RM No. E7A17, Bur. Aero., 1947.

## INDEX OF FIGURES

- Figure 1. - Power-plant installation of XR60 airplane in altitude wind tunnel.
- Figure 2. - Induction system of power-plant installation for XR60 airplane.
- Figure 3. - Exhaust system of power-plant installation for XR60 airplane.
- Figure 4. - Pressure-recovery pattern at main-duct inlet. Altitude, 10,000 feet; intercooler-flap deflection,  $0^\circ$  to  $1^\circ$  from faired position; indicated airspeed, 150 miles per hour.
- (a) Propeller removed.
  - (b) Propeller operating: brake horsepower, 1675; engine speed, 2230 rpm.
  - (c) Propeller operating: brake horsepower, 2500; engine speed, 2550 rpm.
- Figure 5. - Variation of average total-pressure recovery at main-duct inlet for various flight conditions.
- (a) Effect of brake horsepower. Altitude, 15,000 feet; indicated airspeed, 150 miles per hour.
  - (b) Effect of altitude at various brake horsepower. Indicated airspeed, 150 miles per hour.
  - (c) Effect of indicated airspeed. Altitude, 15,000 feet; brake horsepower, 1675; engine speed, 2230 rpm.
- Figure 6. - Pressure-recovery patterns at entrance to separate intake ducts. Altitude, 10,000 feet; indicated airspeed, 150 miles per hour.
- Figure 7. - Variation of pressure-drop coefficient between main-duct inlet and intercooler-duct inlets with charge-air flow. Altitude, 15,000 feet; intercooler-flap deflection,  $0^\circ$  to  $1^\circ$  from faired position; indicated airspeed, 150 miles per hour.
- (a) Engine speed, 2700 rpm.
  - (b) Engine speed, 2400 rpm.
  - (c) Engine speed, 2230 rpm.
- Figure 8. - Pressure-recovery patterns at charge-air duct inlet. Front view; altitude, 10,000 feet; indicated airspeed, 150 miles per hour.
- (a) Propeller removed.
  - (b) Propeller operating: brake horsepower, 2500; engine speed, 2550 rpm.

Figure 9. - Total-pressure gradient of engine charge air through induction system. Intercooler-flap deflection,  $0^\circ$  to  $1^\circ$  from faired position; indicated airspeed, 150 miles per hour.

- (a) Effect of brake horsepower. Altitude, 15,000 feet.
- (b) Effect of altitude. Brake horsepower, 1675; engine speed, 2230 rpm.

Figure 10. - Temperature gradient of engine charge air through induction system. Intercooler-flap deflection,  $0^\circ$  to  $1^\circ$  from faired position; indicated airspeed, 150 miles per hour.

- (a) Effect of brake horsepower. Altitude, 15,000 feet.
- (b) Effect of altitude. Brake horsepower, 1675; engine speed, 2230 rpm.

Figure 11. - Variation of total-pressure loss throughout charge-air system with brake horsepower. Altitude, 15,000 feet; indicated airspeed, 150 miles per hour.

Figure 12. - Charge-air pressure distribution at intercooler inlet. Bottom view; altitude, 15,000 feet; brake horsepower, 2950; engine speed, 2690 rpm.

- (a) Left intercooler.
- (b) Right intercooler.

Figure 13. - Total-pressure distribution at carburetor top deck. Altitude, 15,000 feet; indicated airspeed, 150 miles per hour.

- (a) Brake horsepower, 3000; engine speed, 2700 rpm.
- (b) Brake horsepower, 1680; engine speed, 2230 rpm.

Figure 14. - Pressure-recovery gradients of intercooler cooling air. Indicated airspeed, 150 miles per hour.

- (a) Effect of brake horsepower. Altitude, 15,000 feet; intercooler-flap deflection,  $0^\circ$  to  $1^\circ$  from faired position.
- (b) Effect of altitude. Brake horsepower, 1675; engine speed, 2230 rpm; intercooler-flap deflection,  $0^\circ$  to  $1^\circ$  from faired position.
- (c) Effect of intercooler-flap deflection. Altitude, 10,000 feet; brake horsepower, 1675; engine speed, 2230 rpm.

Figure 15. - Temperature gradients of intercooler cooling air. Indicated airspeed, 150 miles per hour.

- (a) Effect of brake horsepower. Altitude, 15,000 feet; intercooler-flap deflection,  $0^\circ$  to  $1^\circ$  from faired position.
- (b) Effect of altitude. Brake horsepower, 1675; engine speed, 2230 rpm; intercooler-flap deflection,  $0^\circ$  to  $1^\circ$  from faired position.
- (c) Effect of intercooler-flap deflection. Altitude, 10,000 feet; brake horsepower, 1675; engine speed, 2230 rpm.

Figure 16. - Pressure-recovery pattern of cooling air at intercooler-inlet face. Altitude, 10,000 feet; indicated airspeed, 150 miles per hour.

(a) Left intercooler.

(b) Right intercooler.

Figure 17. - Variation in total-pressure drop of cooling air through intercooler and incremental drag with intercooler-flap deflection. Altitude, 10,000 feet; cowl flap and oil-cooler flap full open.

Figure 18. - Effect of intercooler-flap deflection on intercooler characteristics with carburetor preheater system. Altitude, 5000 feet; brake horsepower, 1240; engine speed, 2000 rpm; indicated airspeed, 150 miles per hour; average cowl-inlet air temperature, 9° F.

Figure 19. - Variation of exhaust back pressure at engine cylinder ports with brake horsepower. Altitude, 5000 feet.

Figure 20. - Static-pressure gradients through exhaust system. Indicated airspeed, 150 miles per hour.

(a) Effect of brake horsepower. Altitude, 15,000 feet.

(b) Effect of altitude. Brake horsepower, 1675; engine speed, 2230 rpm.

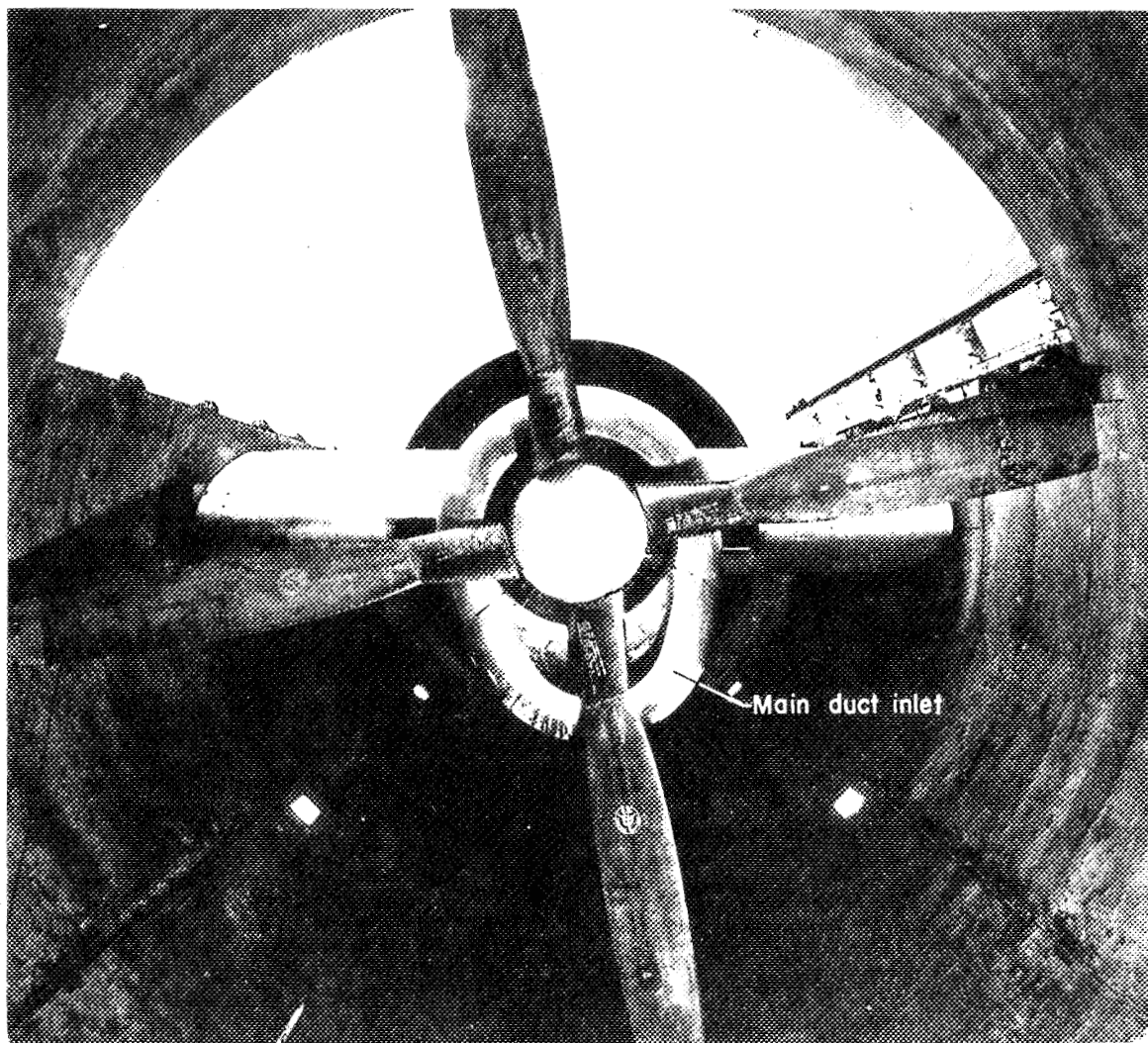


Figure 1. - Power-plant installation of XR60 airplane in altitude wind tunnel.

NACA  
C-13649  
11-16-45

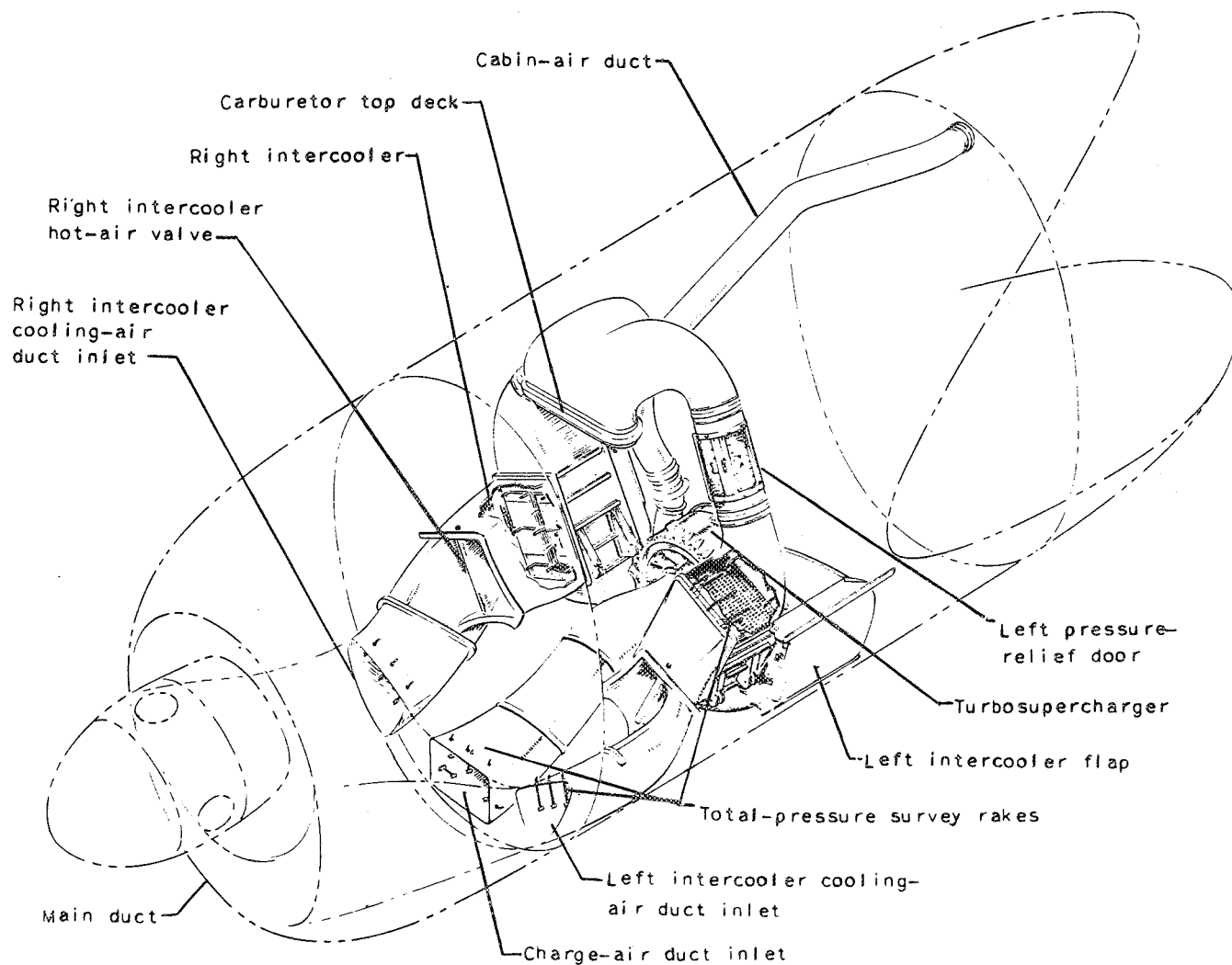
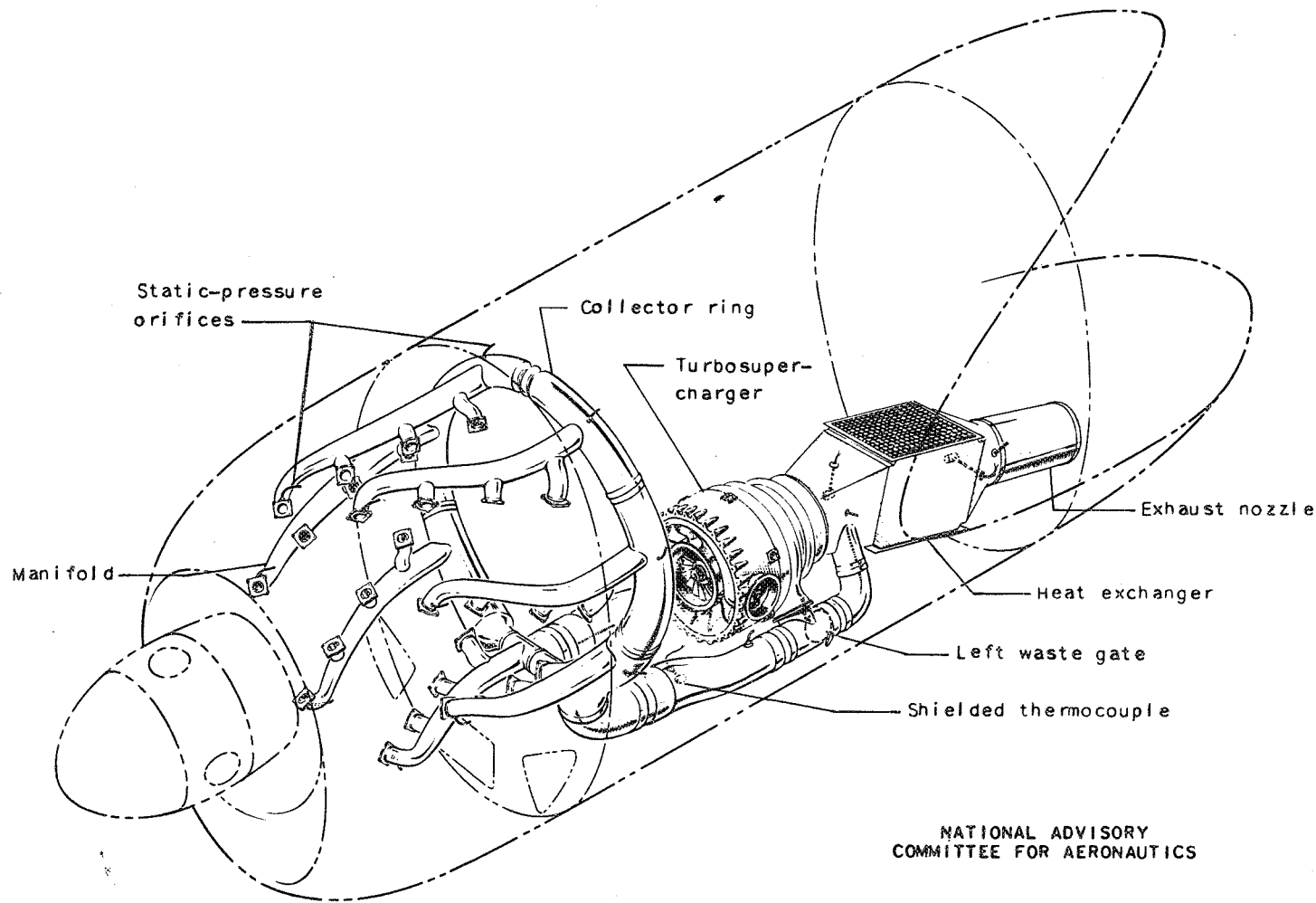


Figure 2. - Induction system of power-plant installation for XR60 airplane.



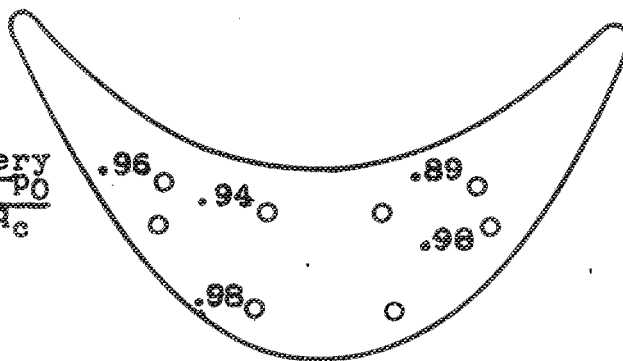


NATIONAL ADVISORY  
COMMITTEE FOR AERONAUTICS

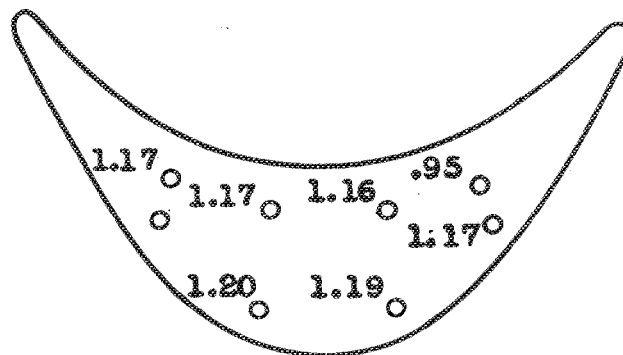
Figure 3. - Exhaust system of power-plant installation for XR60 airplane.

NATIONAL ADVISORY  
COMMITTEE FOR AERONAUTICS

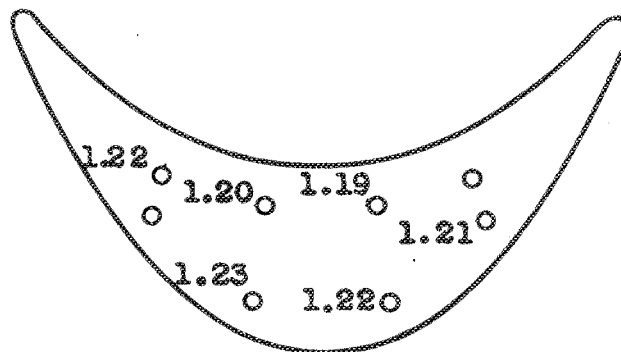
Pressure-recovery  
coefficient,  $\frac{H-P_0}{\frac{\rho}{2} V_c^2}$



(a) Propeller removed.

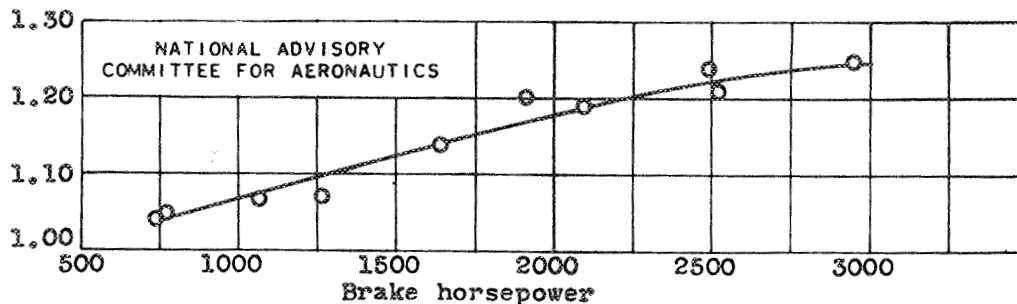


(b) Propeller operating: brake horsepower, 1675;  
engine speed, 2230 rpm.

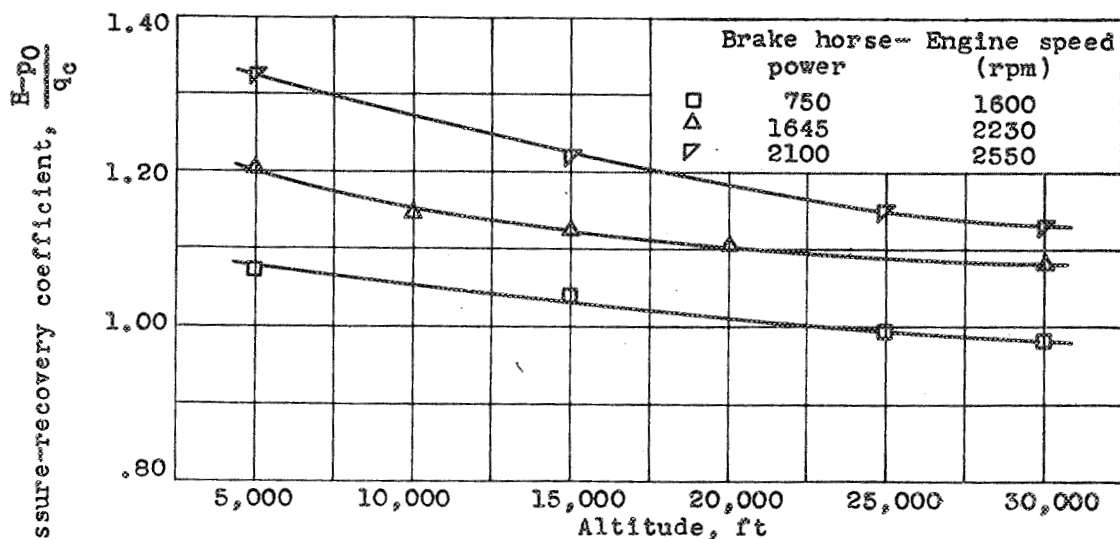


(c) Propeller operating: brake horsepower, 2500;  
engine speed, 2550 rpm.

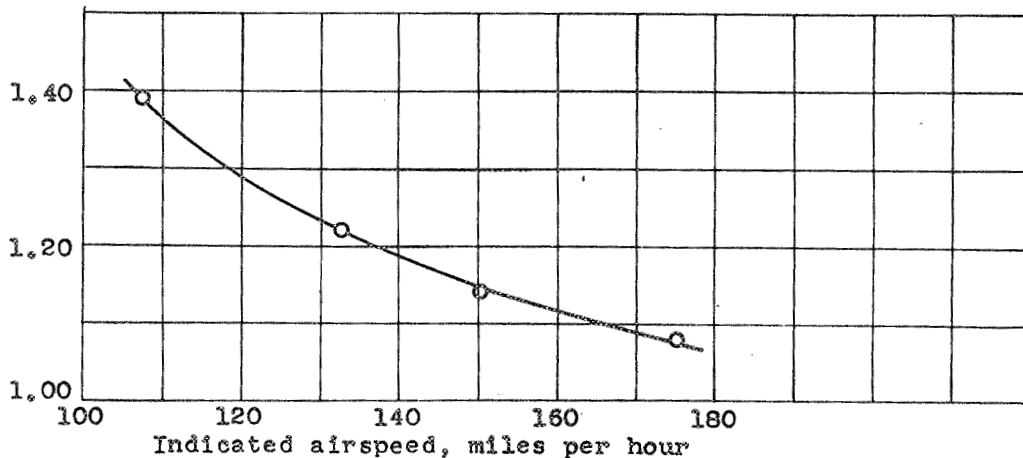
Figure 4.- Pressure-recovery pattern at main-duct inlet. Altitude, 10,000 feet; intercooler-flap deflection, 0° to 1° from faired position; indicated airspeed, 150 miles per hour.



(a) Effect of brake horsepower. Altitude, 15,000 feet; indicated airspeed, 150 miles per hour.



(b) Effect of altitude at various brake horsepower; indicated airspeed, 150 miles per hour.



(c) Effect of indicated airspeed. Altitude, 15,000 feet; brake horsepower, 1675; engine speed, 2230 rpm.

Figure 5.- Variation of average total-pressure recovery at main-duct inlet for various flight conditions.

NATIONAL ADVISORY  
COMMITTEE FOR AERONAUTICS

	Brake horse- power	Engine speed (rpm)
○	Propeller removed	
◇	1475	1900
△	1675	2230
▽	2500	2550

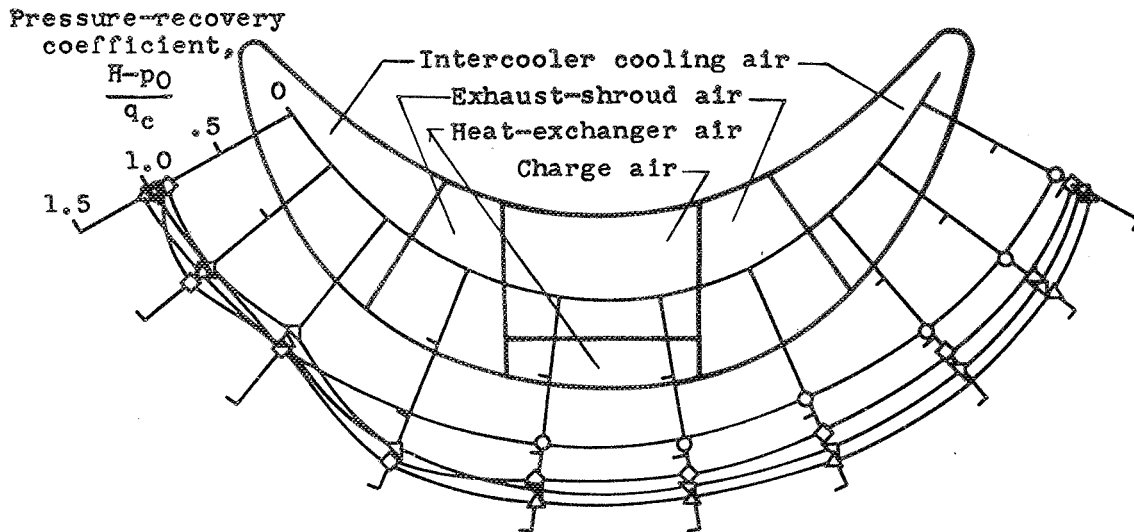
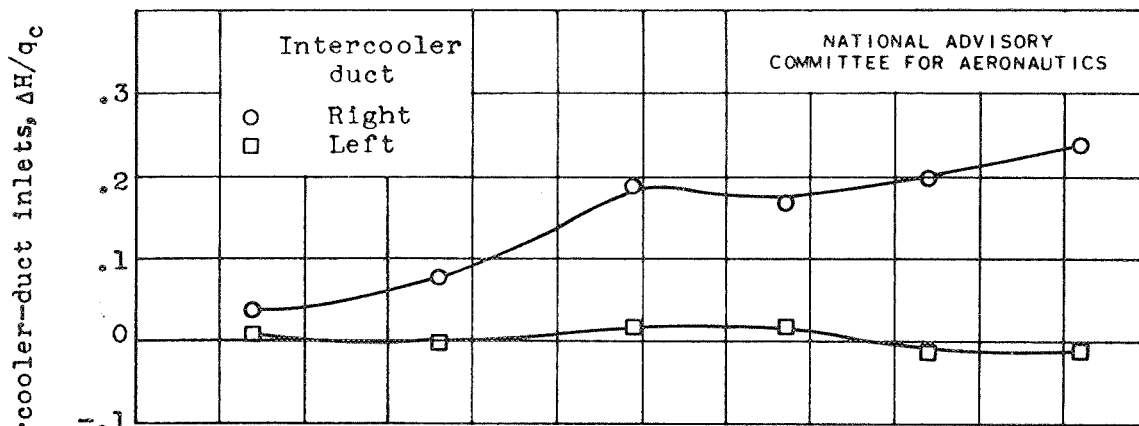
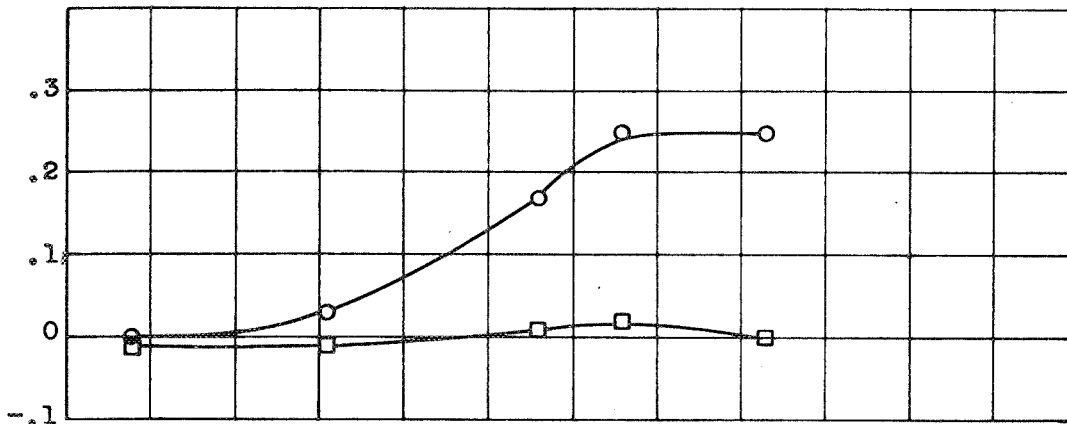


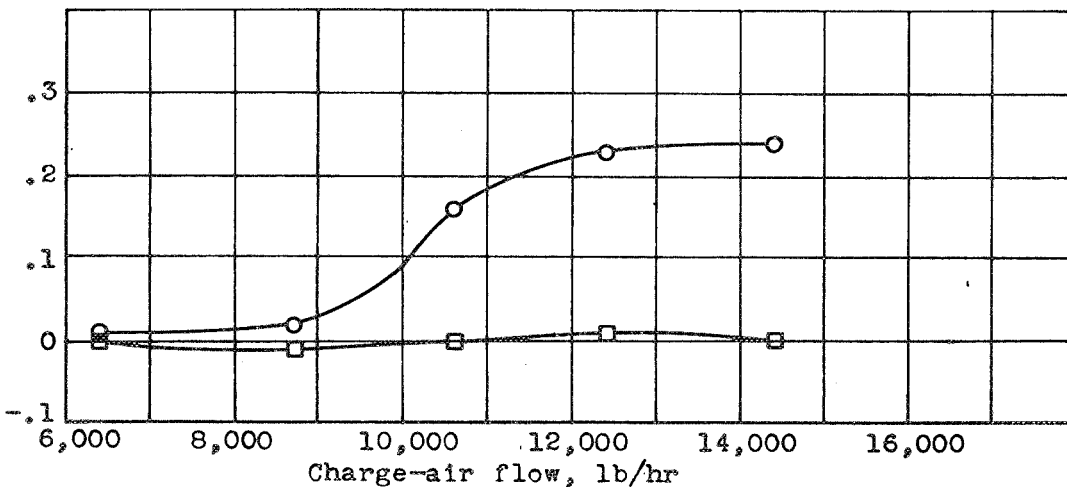
Figure 6.- Pressure-recovery patterns at entrance to separate inlet ducts. Altitude, 10,000 feet; indicated airspeed, 150 miles per hour.



(a) Engine speed, 2700 rpm.



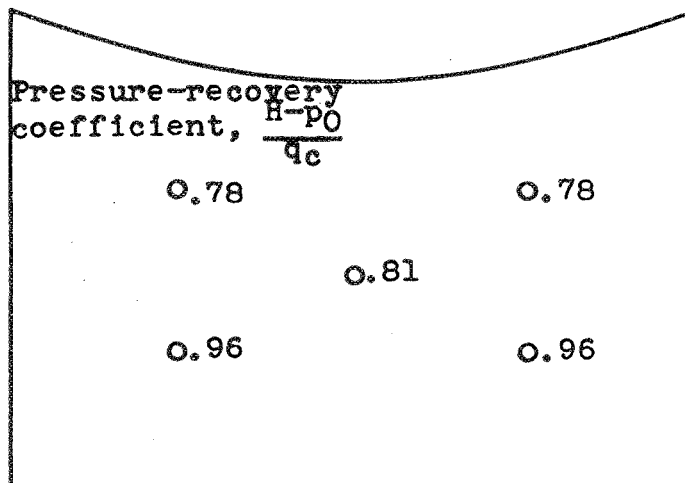
(b) Engine speed, 2400 rpm.



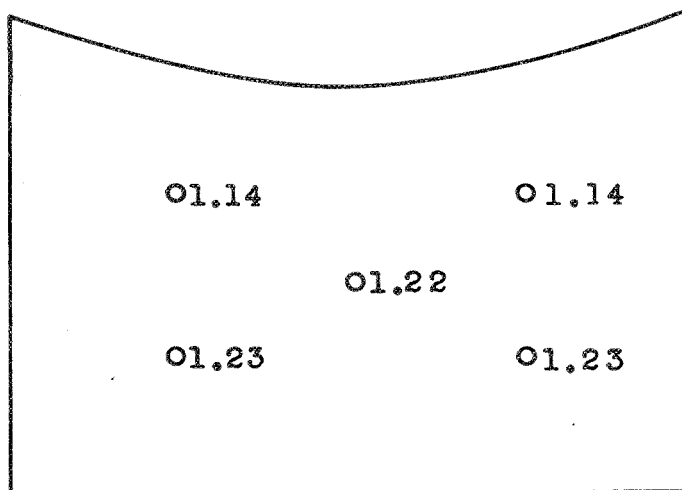
(c) Engine speed, 2230 rpm.

Figure 7.- Variation of pressure-drop coefficient between main-duct inlet and intercooler-duct inlets with charge-air flow. Altitude, 15,000 feet; intercooler-flap deflection, 0° to 1° from faired position; indicated airspeed, 150 miles per hour.

NATIONAL ADVISORY  
COMMITTEE FOR AERONAUTICS

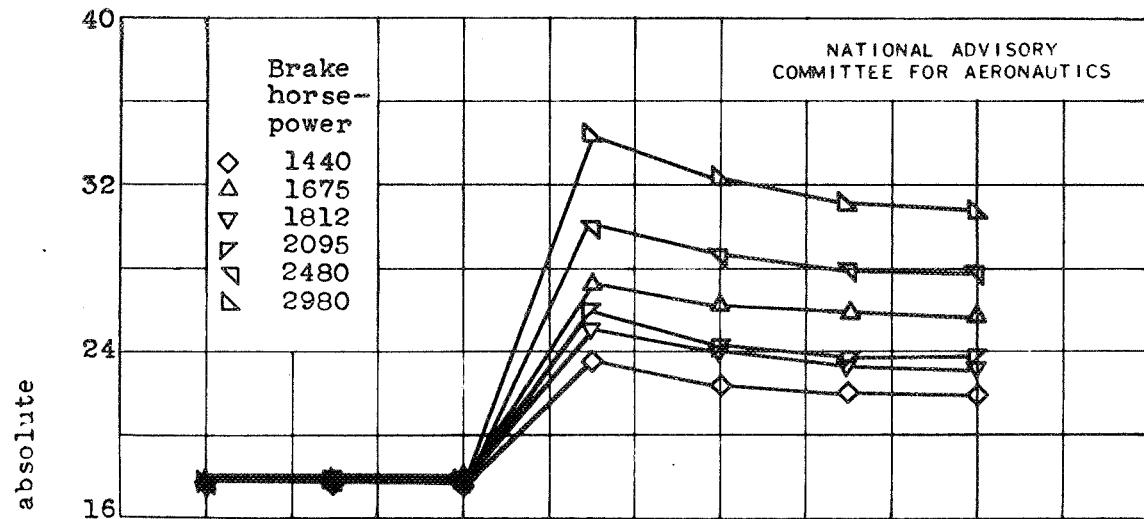


(a) Propeller removed.

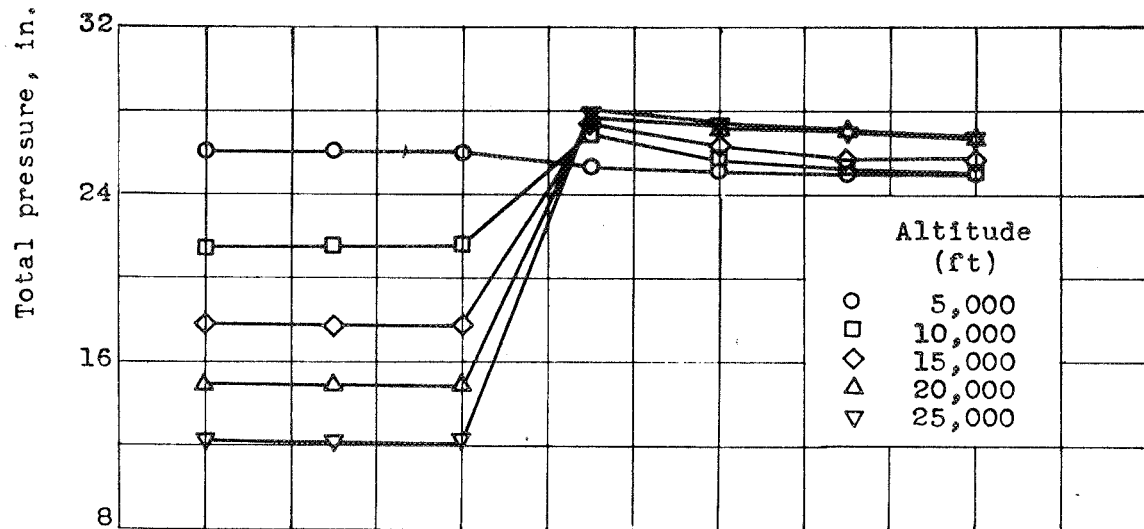


(b) Propeller operating: brake horsepower, 2500;  
engine speed, 2550 rpm.

Figure 8.- Pressure-recovery patterns at charge-air duct inlet. Front view; altitude, 10,000 feet; indicated airspeed, 150 miles per hour.



(a) Effect of brake horsepower. Altitude, 15,000 feet.



(b) Effect of altitude. Brake horsepower, 1675; engine speed, 2230 rpm.

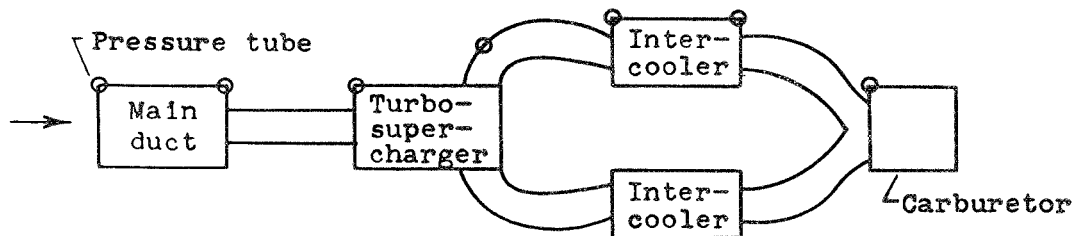
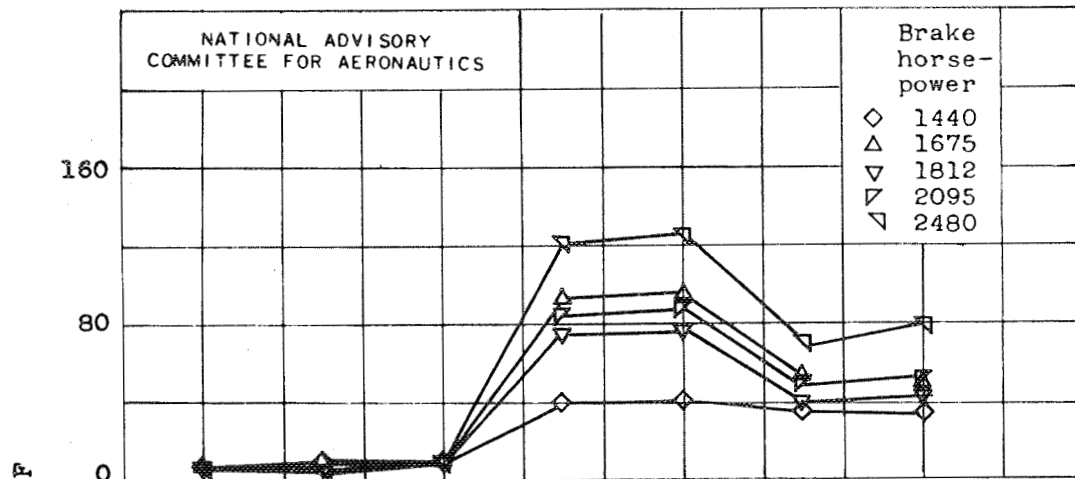
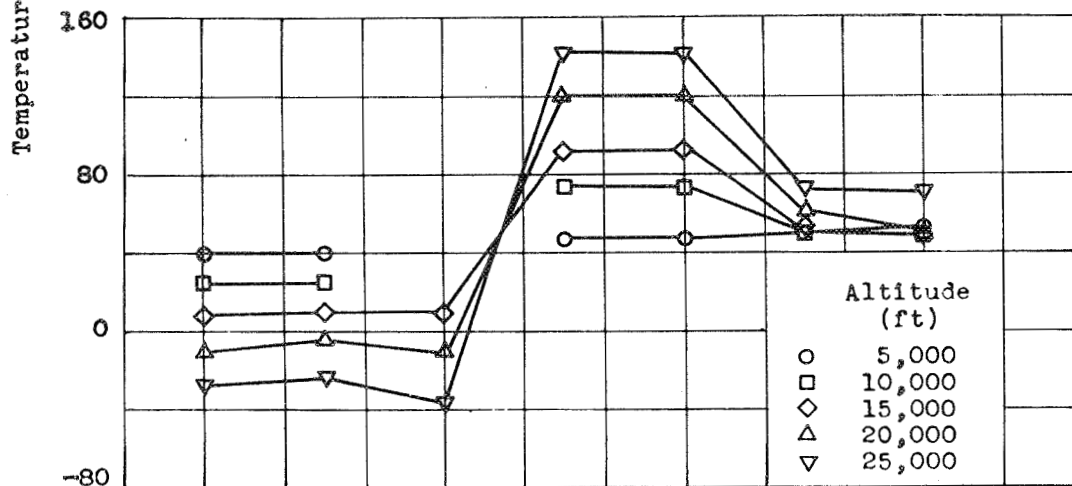


Figure 9.- Total-pressure gradient of engine charge air through induction system. Intercooler-flap deflection, 0° to 1° from faired position; indicated airspeed, 150 miles per hour.



(a) Effect of brake horsepower. Altitude, 15,000 feet.



(b) Effect of altitude. Brake horsepower, 1675; engine speed, 2230 rpm.

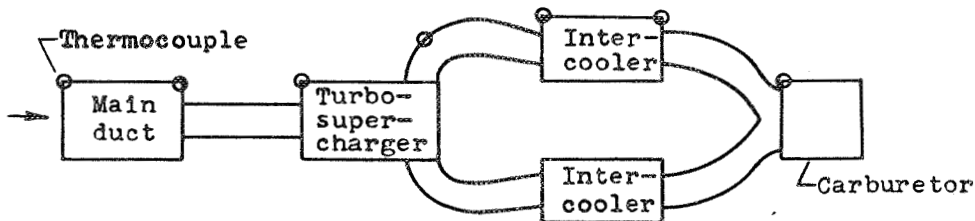


Figure 10.- Temperature gradient of engine charge air through induction system. Intercooler-flap deflection, 0° to 1° from faired position; indicated airspeed, 150 miles per hour.



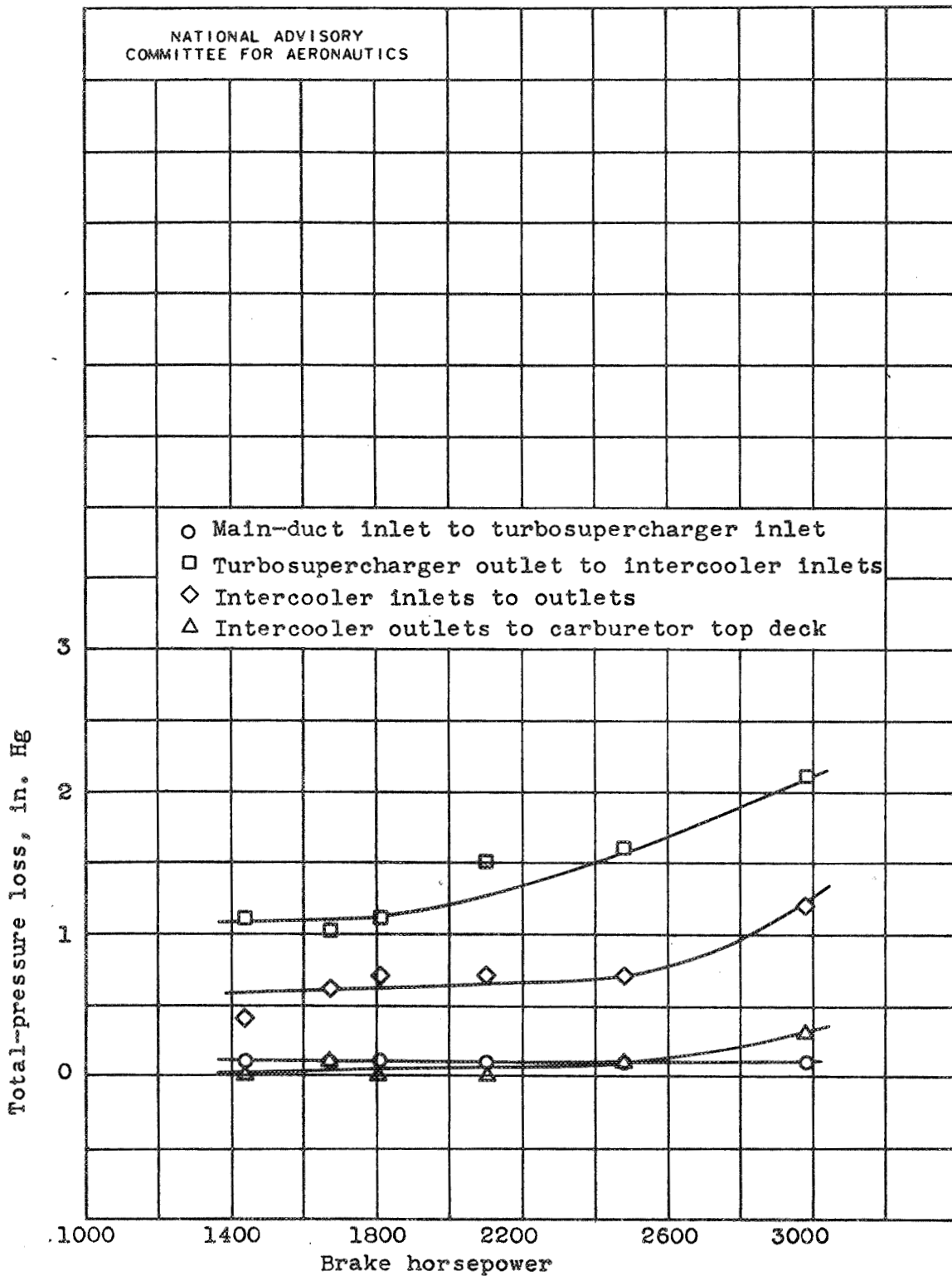
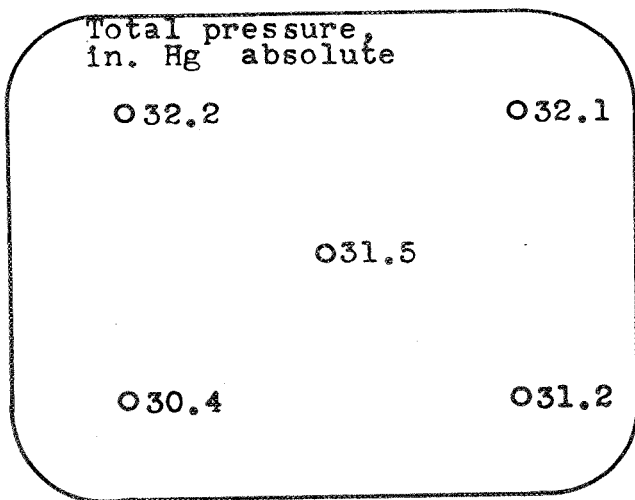


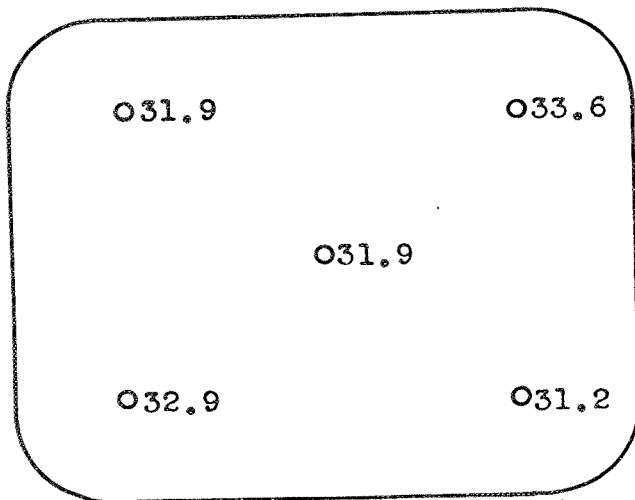
Figure 11.- Variation of total-pressure loss throughout charge-air system with brake horsepower. Altitude, 15,000 feet; indicated airspeed, 150 miles per hour.



(a) Left intercooler.



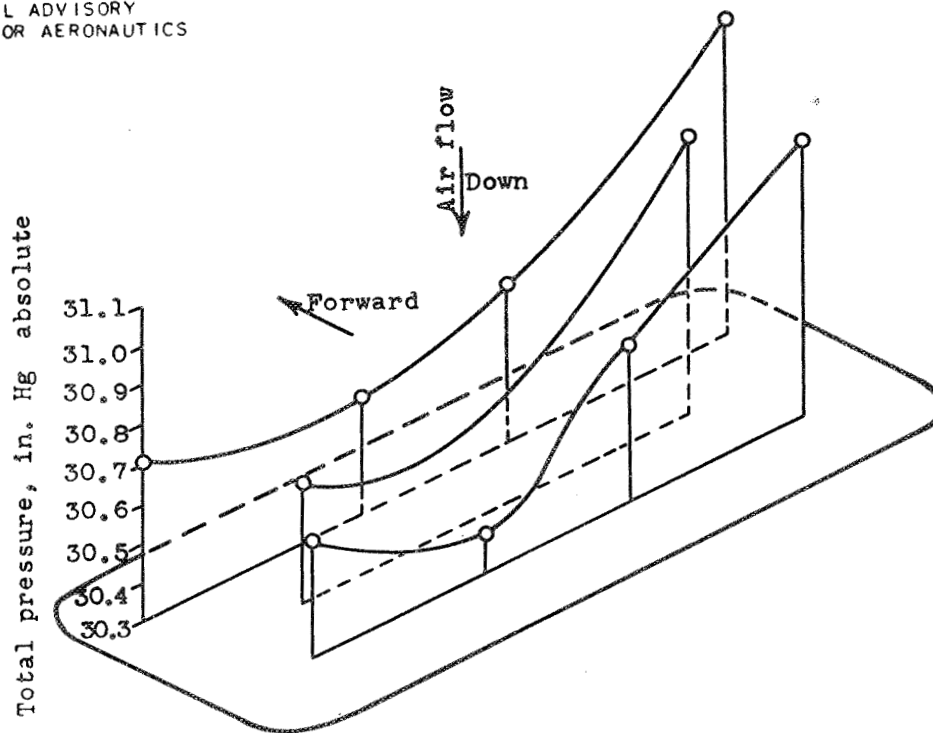
NATIONAL ADVISORY  
COMMITTEE FOR AERONAUTICS



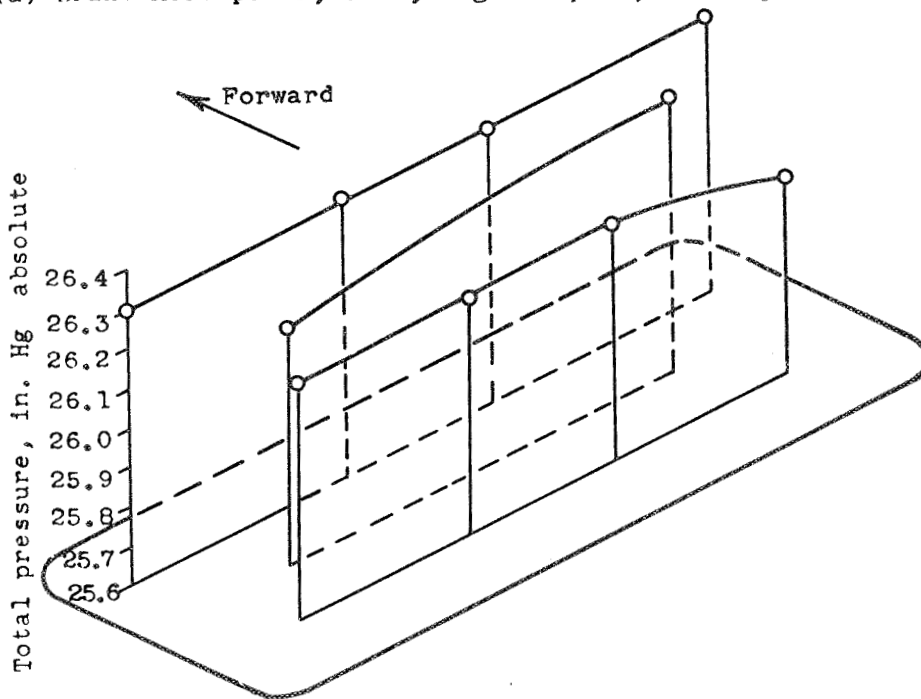
(b) Right intercooler.

Figure 12.- Charge-air pressure distribution at intercooler inlet. Bottom view; altitude, 15,000 feet; brake horsepower, 2950; engine speed, 2690 rpm.

NATIONAL ADVISORY  
COMMITTEE FOR AERONAUTICS

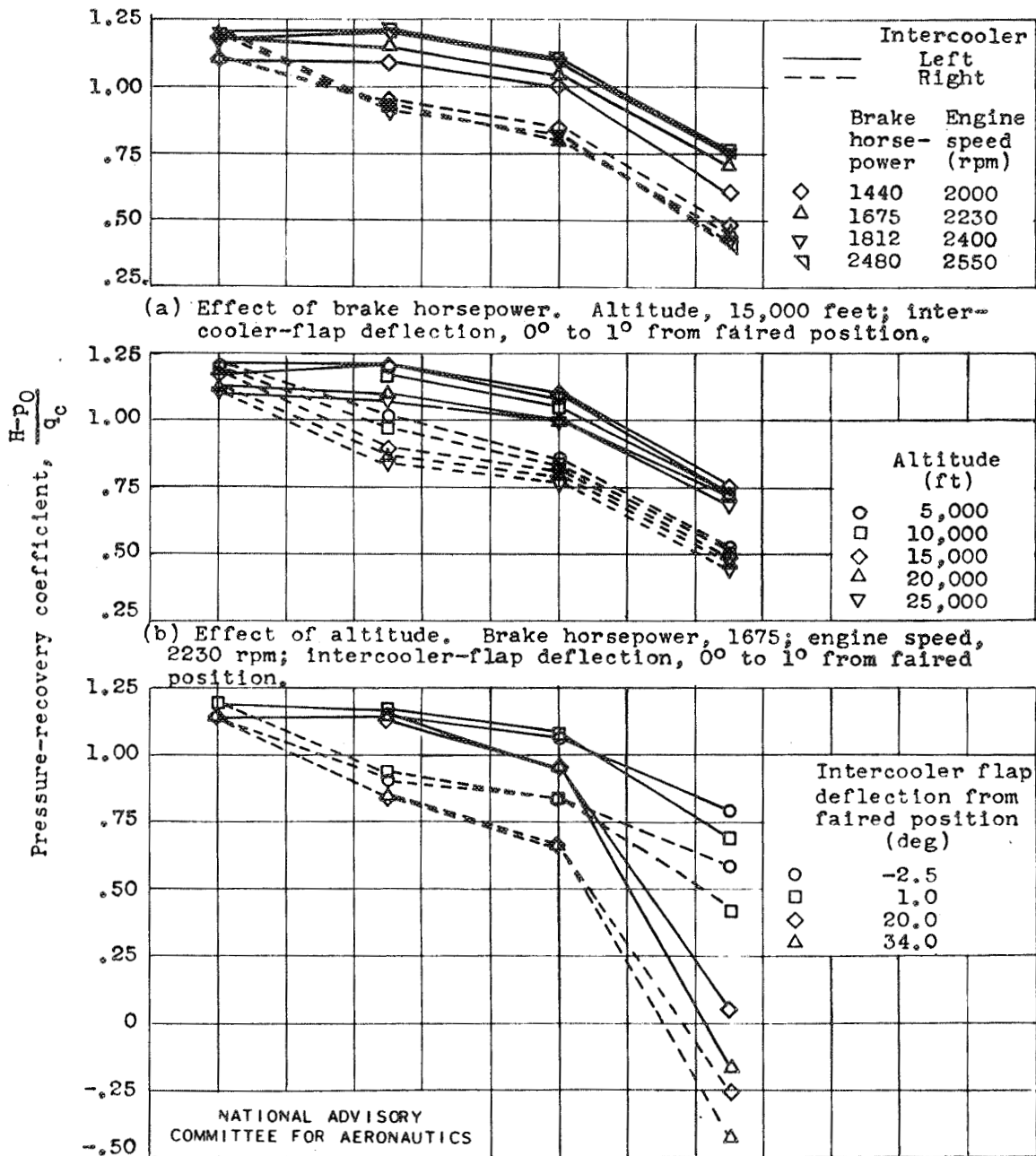


(a) Brake horsepower, 3000; engine speed, 2700 rpm.



(b) Brake horsepower, 1680; engine speed, 2230 rpm.

Figure 13.- Total-pressure distribution at carburetor top deck. Altitude, 15,000 feet; indicated airspeed, 150 miles per hour.



(c) Effect of intercooler-flap deflection. Altitude, 10,000 feet; brake horsepower, 1675; engine speed, 2230 rpm.

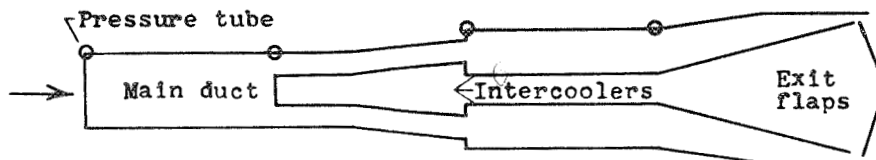


Figure 14.- Pressure-recovery gradients of intercooler cooling air. Indicated airspeed, 150 miles per hour.

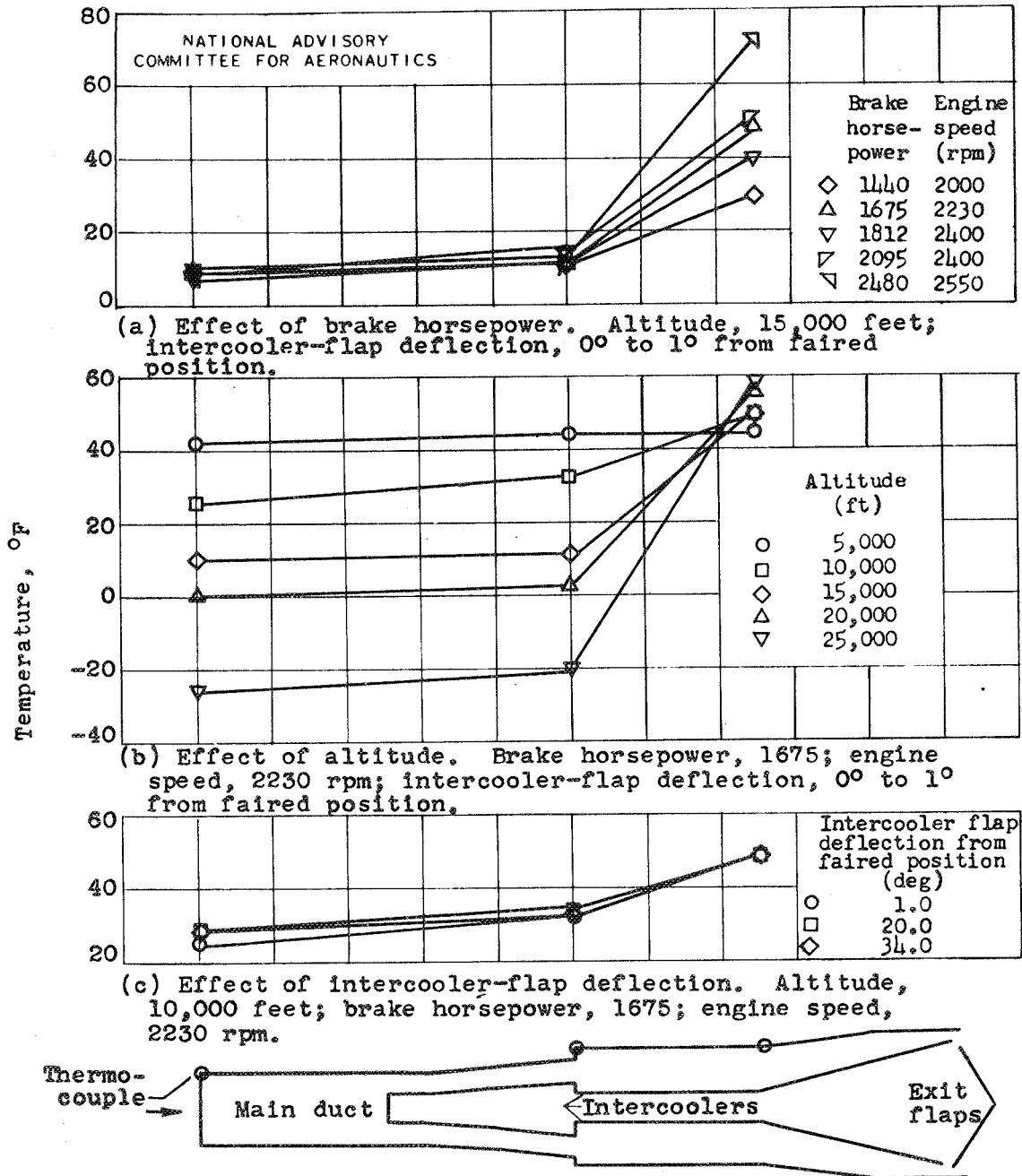
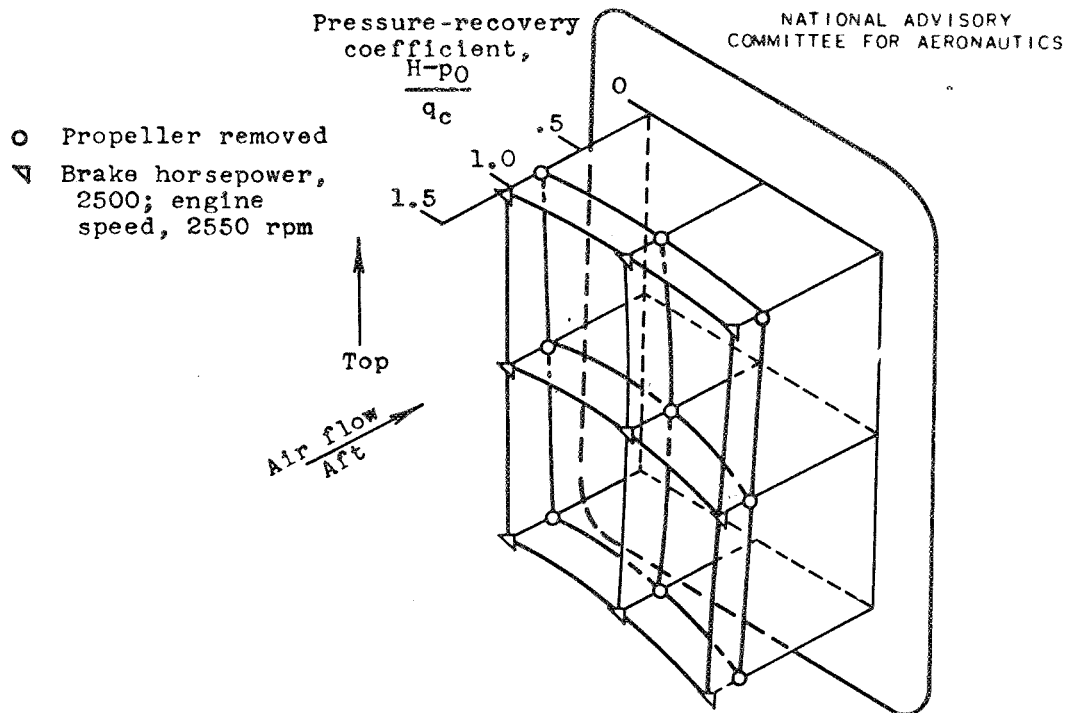
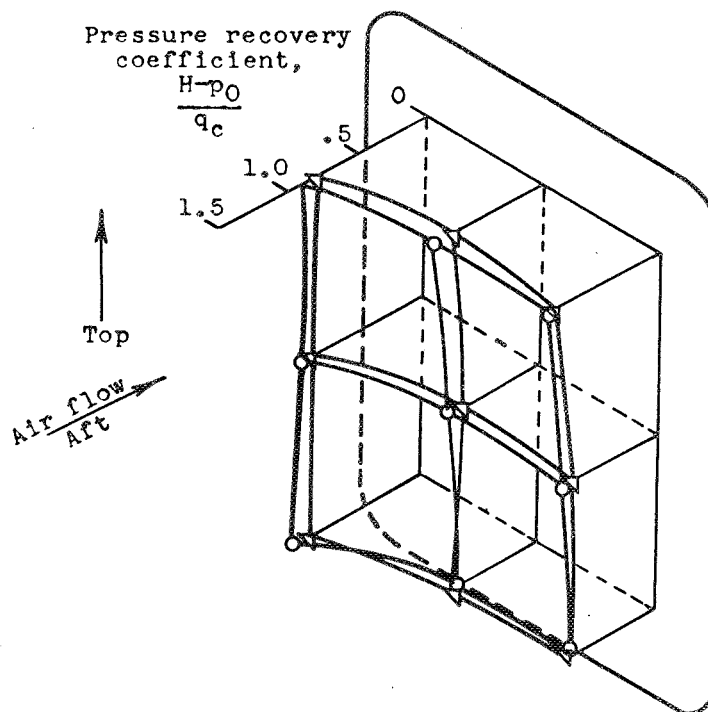


Figure 15.- Temperature gradients of intercooler cooling air. Indicated airspeed, 150 miles per hour.



(a) Left intercooler.



(b) Right intercooler.

Figure 16.- Pressure-recovery pattern of cooling air at intercooler-inlet face. Altitude, 10,000 feet; indicated airspeed, 150 miles per hour.

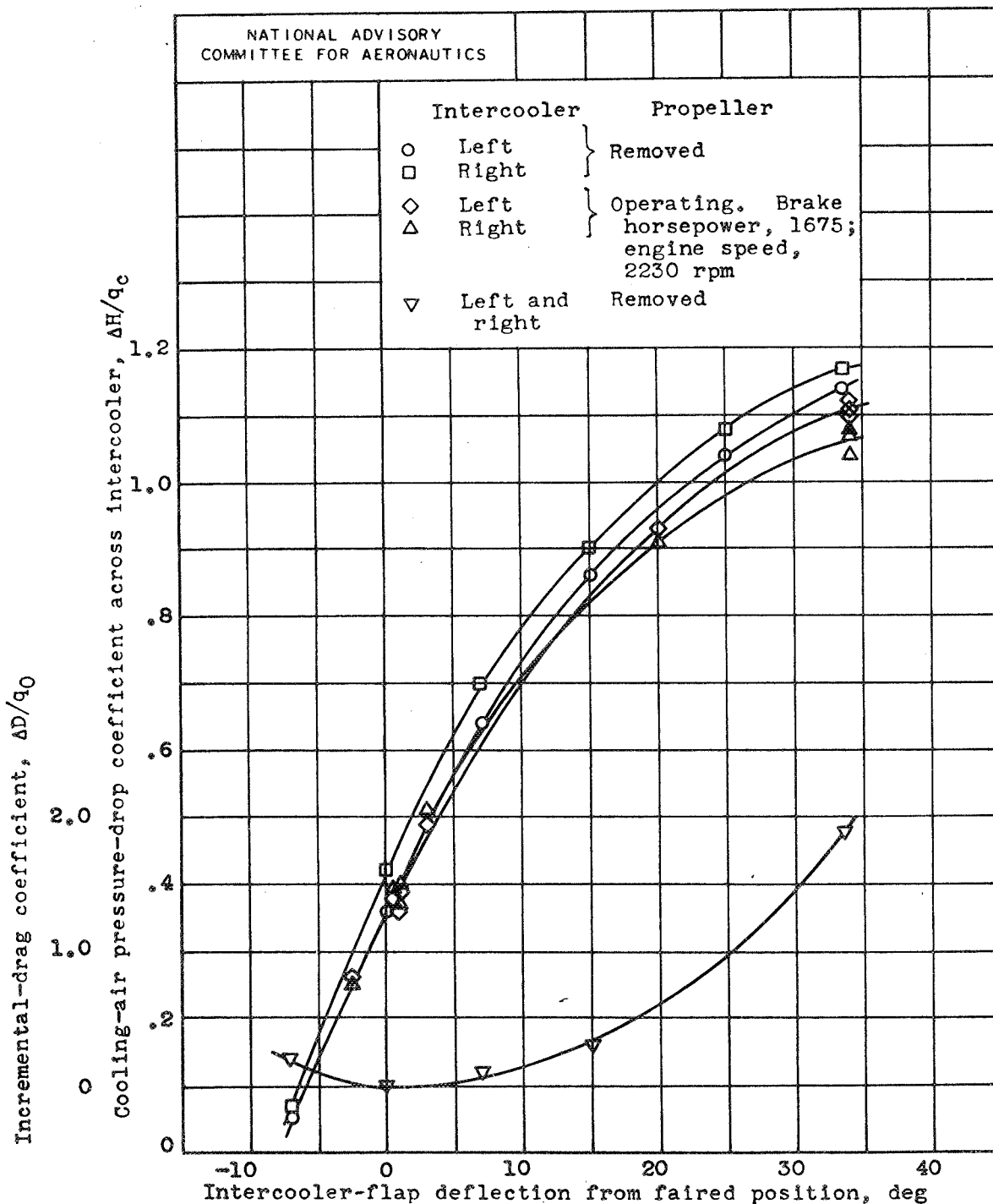


Figure 17.- Variation in total-pressure drop of cooling air through intercooler and incremental drag with intercooler-flap deflection. Altitude, 10,000 feet; cowl flap and oil-cooler flap full open.

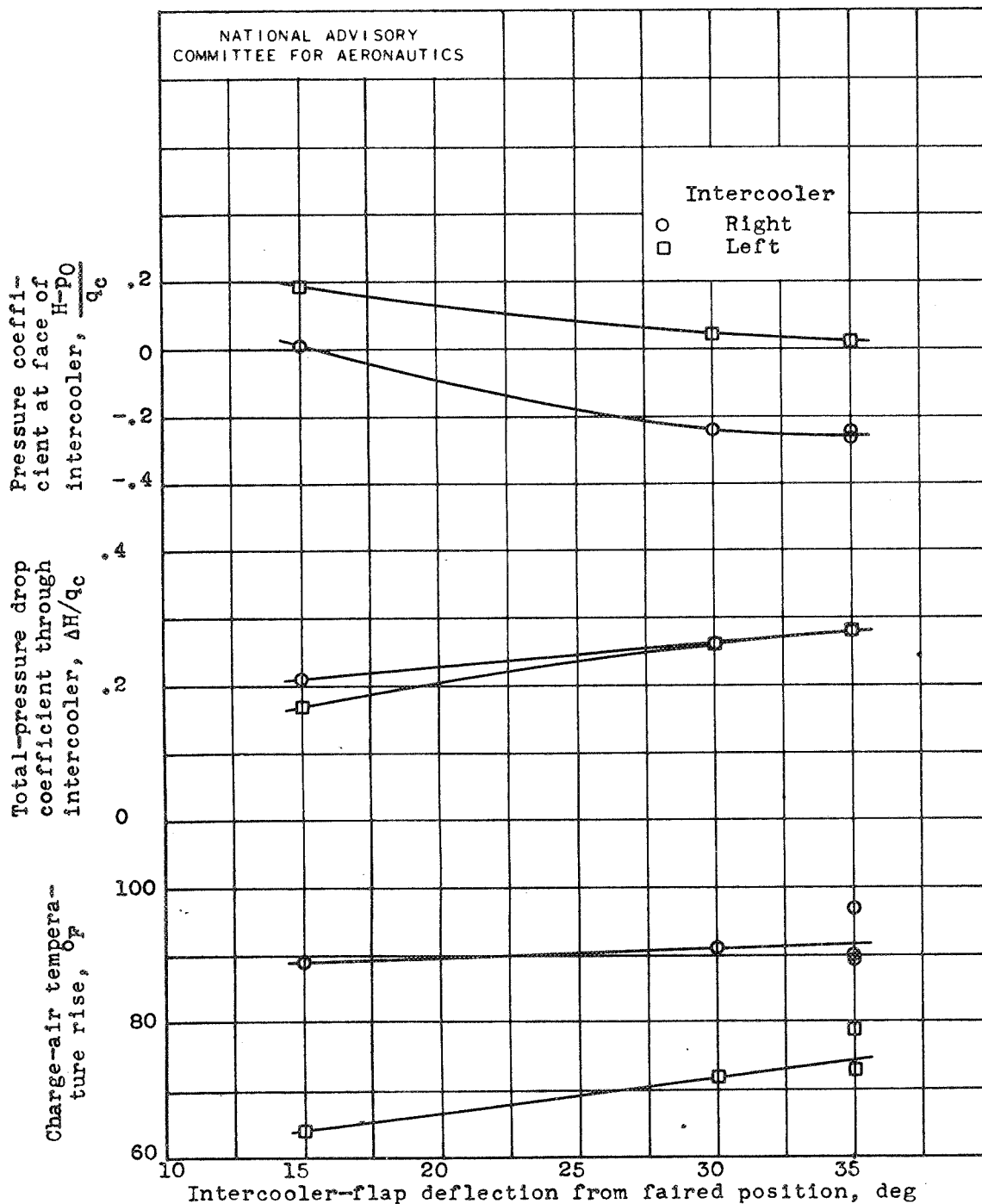


Figure 18.- Effect of intercooler-flap deflection on intercooler characteristics with carburetor preheater system. Altitude, 5000 feet; brake horsepower, 1240; engine speed, 2000 rpm; indicated airspeed, 150 miles per hour; average cowl-inlet air temperature, 90 F.



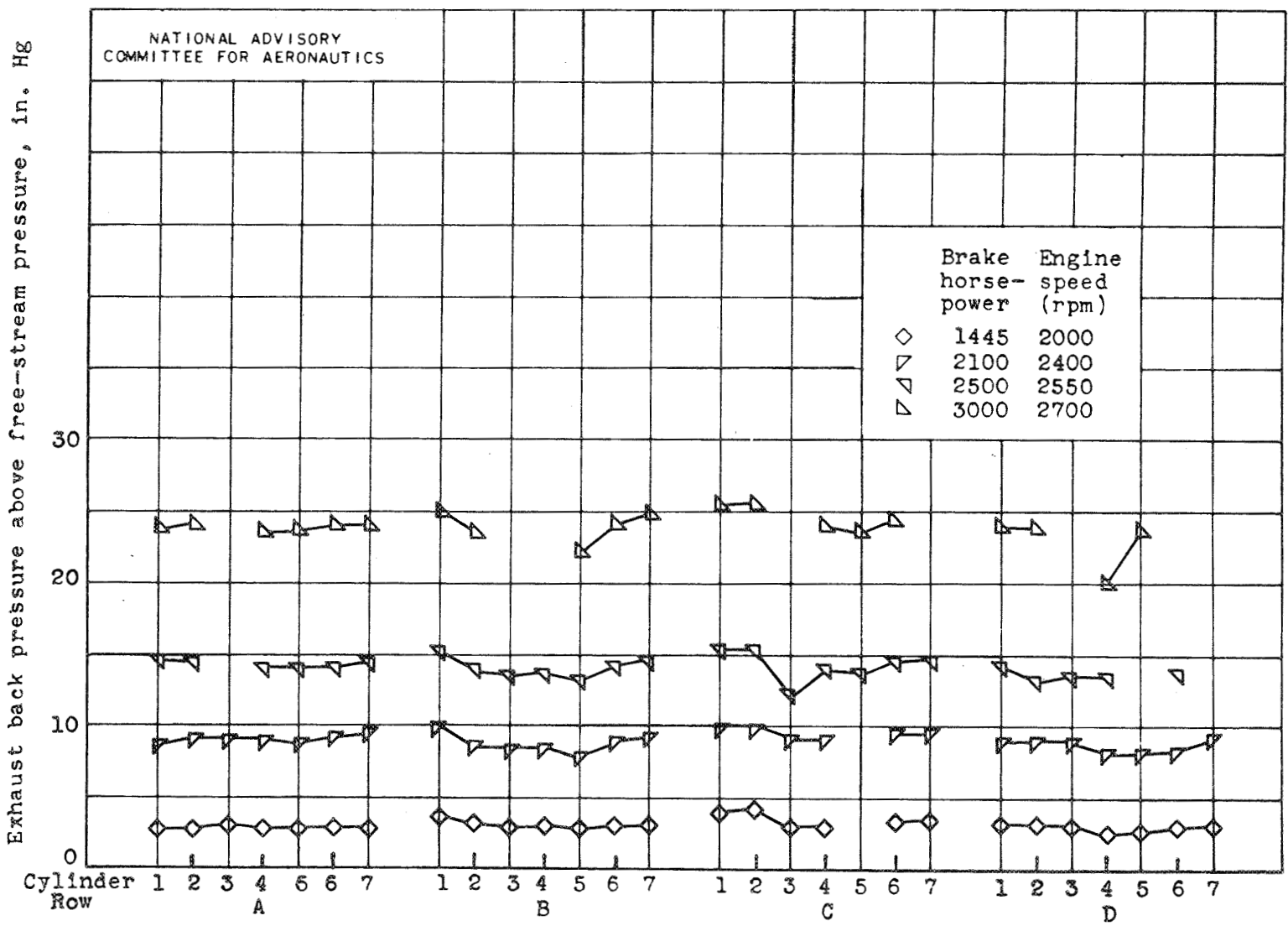
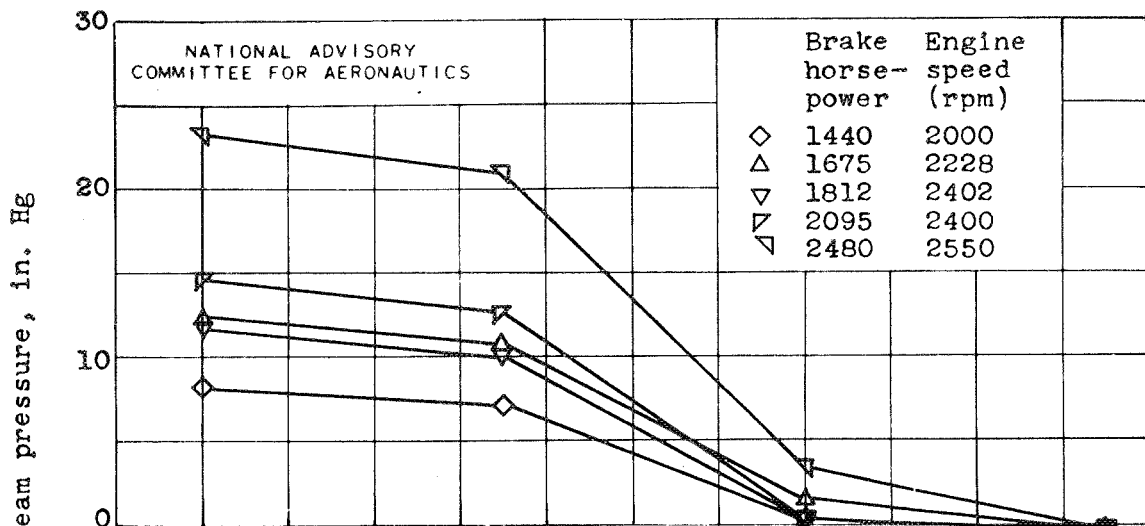
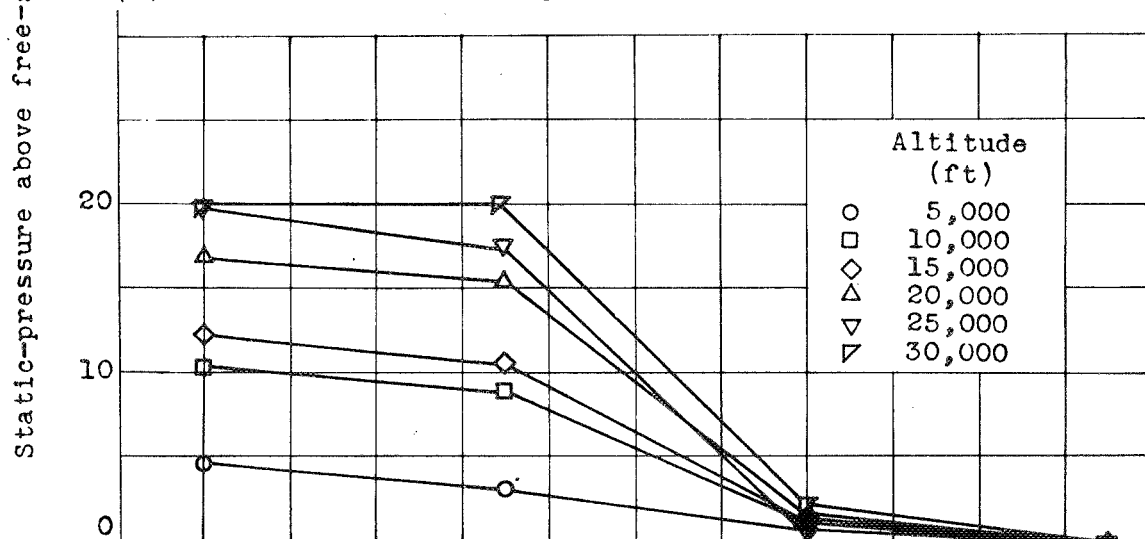


Figure 19.- Variation of exhaust back pressure at engine cylinder ports with brake horsepower. Altitude, 5000 feet.



(a) Effect of brake horsepower. Altitude, 15,000 feet.



(b) Effect of altitude. Brake horsepower, 1675; engine speed, 2230 rpm.

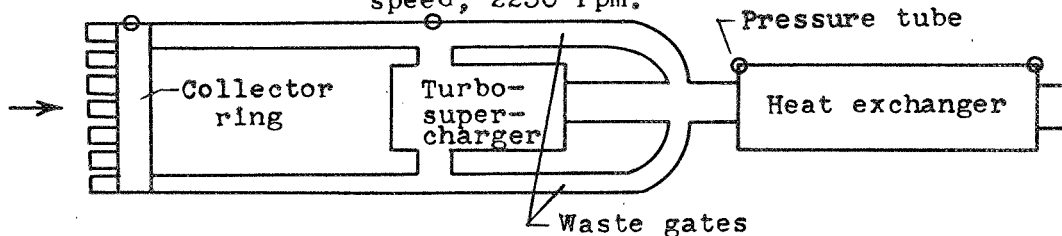


Figure 20.- Static-pressure gradients through exhaust system. Indicated airspeed, 150 miles per hour.